Is Cytochrome *b* Glutamic Acid 272 a Quinol Binding Residue in the bc_1 Complex of *Saccharomyces cerevisiae*?

Nadir Seddiki,[‡,§] Brigitte Meunier,[‖] Danielle Lemesle-Meunier,[‡] and Gaël Brasseur*[,‡]

Laboratoire de Bioénergétique et Ingénierie des Protéines, CNRS, 31 Chemin Joseph Aiguier, 13402 Marseille cedex 20, France, and Centre de Génétique Moléculaire, CNRS, UPR 2167, Gif-sur-Yvette, F-91198, France

Received September 18, 2007; Revised Manuscript Received December 14, 2007

ABSTRACT: The mitochondrial bc_1 complex catalyzes the oxidation of ubiquinol and the reduction of cytochrome (cyt) *c* coupled to a vectorial translocation of protons across the membrane. On the basis of the three-dimensional structures of the bc_1 complex in the presence of the inhibitor stigmatellin, it was assumed that the substrate quinol binding involves the cyt *b* glutamate residue E272 and the histidine 181 on the Rieske protein. Although extensive mutagenesis of glutamate E272 has been carried out, different experimental results were recently obtained, and different conclusions were drawn to explain its role in the bifurcated electron/proton transfer at the Q_O site. This residue is not totally conserved during evolution. We show in this study that replacement of E272 with apolar residues proline and valine naturally present in some organisms did not abolish the bc_1 activity, although it slowed down the kinetics of electron transfer. The K_m value for the binding of the substrate quinol was not modified, and the EPR data showed that the quinone/quinol binding still occurred in the mutants. Binding of stigmatellin was retained; however, mutations E272P,V induced resistance toward the Q_O site inhibitor myxothiazol. The pH dependence of the bc_1 activity was not modified in the absence of the glutamate E272. Our results suggest that this residue may not be involved in direct substrate binding or in its direct deprotonation. Revertants were selected from the respiratory deficient mutant E272P. The observed suppressor mutations introduced polar residues serine and threonine at position 272. The data lead us to suggest that E272 may be involved in a later step on the proton exit pathway via the interaction with a water molecule.

The cytochrome bc_1 complex (known as the b_6f complex in chloroplasts and cyanobacteria) is a key component of respiratory and photosynthetic electron transfer chains (see refs *1*−*6* for reviews). It is present in the inner mitochondrial membrane of eukaryotes and in the cytoplasmic membrane of bacteria and catalyzes the oxidation of the two electrons and two proton carriers of ubiquinol linked to the reduction of cytochrome (cyt)[1] *c*. This electron transfer is coupled to a vectorial translocation of protons across the membrane and is best described by the Q cycle mechanism (*7*−*10*). Although the general mechanism of the bc_1 complex is well-described, several models have been proposed using the Q cycle framework to account for the bifurcated electron transfer at the Q_P site (*8*, *9*, *11*−*20*). Almost all bc_1 complexes, from bacteria to higher eukaryotes, contain three subunits forming the catalytic core of the enzyme and carrying four prosthetic groups: a FeS Rieske protein (ISP) with a [2Fe-2S] cluster and a monohemic cyt c_1 and a dihemic cyt *b* with a low potential b_L heme ($E_{m7} = -50$ mV) located on the positive side of the membrane and a high potential b_H heme ($E_{m7} = +90$ mV) located on the negative side of the membrane. In eukaryotes, in addition to these three conserved subunits, up to eight additional subunits are present whose functions are poorly understood (*21*).

Several three-dimensional structures of bacterial and eukaryotic bc_1/b_6f complexes have been obtained in the presence or absence of different inhibitors (*18*, *22*−*29*). On the basis of these structural data and experimental results, the extrinsic domain of the ISP carrying the [2Fe-2S] cluster was shown to undergo during catalysis a rotation between a position close to cyt *b* (proximal conformation or *b* state) and a position close to cyt c_1 (distal conformation or c_1 state) via a flexible linker domain (*23*−*26*, *30*−*38*). Hunte et al. solved the bc_1 complex structure of the yeast *Saccharomyces cerevisiae* at 2.3 Å including water molecules (*26*), some of which may be crucial for the proton exit and entry pathways on the Q_O and Q_I sites, respectively.

Cyt *b* is an integral membrane protein with eight transmembrane helices and is a central component for quinol oxidation and inhibitor binding. Among the cyt *b* residues that are conserved during evolution, the $PE_{272}WY$ motif is

* To whom correspondence should be addressed. Tel.: +33 (0)4-91-16-45-56; fax: +33 (0)4-91-16-45-40; e-mail: brasseur@ibsm.cnrs-mrs.fr.

‡ Laboratoire de Bioénergétique et Ingénierie des Protéines, CNRS.

§ Present address: Laboratory of Molecular Biology, NIDDK, NIH, 50 South Drive, Bethesda, MD 20892-8030.

‖ Centre de Génétique Moléculaire, CNRS.

[1] Abbreviations: cyt, cytochrome; b_L, low potential cyt *b* heme; b_H, high potential cyt *b* heme; ISP, iron sulphur protein; DB, 2.3-dimethoxy-5-methyl-6-decyl-1.4-benzoquinone; DBH_2, reduced form of DB; UHDBT, 5-*n*-undecyl-6-hydroxy-4,7-dioxobenzothiazole; HHDBT, 5-*n*-heptyl-6-hydroxy-4,7-dioxobenzothiazole; Q_O, ubiquinol oxidation site on the positive side of the inner mitochondrial membrane; Q_I, ubiquinone reduction site on the negative side of the inner mitochondrial membrane; EPR, electron paramagnetic resonance; E_m, equilibrium redox midpoint potential; WT, parental strain.

10.1021/bi701905a CCC: $40.75
Published on Web 01/24/2008

located in the *ef* loop, within the Q_O site, on the positive side of the membrane. Before the atomic structures of the different bc_1/b_6f complexes were known, this motif was the subject of mutagenesis experimentation (*39*, *40*). The authors reported that the conservative mutation E295D in *Rhodobacter sphaeroides* (equivalent to position 272 in yeast) induces a 50% decrease in the quinol oxidation, whereas the QH2 oxidation was slowed down 9- and 50-fold in mutants E295G and E295Q, respectively. Zito et al. (*41*) showed that in the b_6f complex from *Chlamydomonas reinhardtii*, mutations E78L, K, Q, N, and D (equivalent to position 272 in yeast) reduced the rate of the oxidation process at the Q_O site to 20−80% of the WT value without affecting the affinity for the plastoquinols. In the atomic structure of the bc_1 complex in the presence of stigmatellin (*23*, *26*), the inhibitor is both hydrogen-bonded to ISP His 181 via its carbonyl group and to E272 of cyt *b* via its hydroxyl group on the polar head (Figure 1). In the absence of any available structural data on the quinol binding site in the Q_O site and based on the structures in the presence of stigmatellin, it is assumed that the substrate quinol binding takes place in a similar way as the inhibitor binding. As two different orientations of the E272 side chain were observed depending on the inhibitors present in the Q_O site, Crofts et al. (*42*) proposed that E272 would be directly involved in the quinol binding and would be the first proton acceptor in cyt *b* from the quinol, His 181 of ISP also being involved in the direct deprotonation of quinol. This model was tested recently by site directed mutagenesis of this glutamate residue (272) in yeast and *Rhodobacter capsulatus* (corresponding residue E295) by two different research groups working with these organisms. Both studies (*44*, *45*) showed that mutations at this position decreased the kinetics of electron transfer to a level that was still compatible with the growth of the microorganisms and still allowed a partial functioning of the bc_1 complex. However, their infrared spectral data, pH dependence of electron transfer reactions, and quinol binding data as indicated by the EPR spectra differed notably. These apparent discrepancies in the experimental data led to different conclusions as to the role of this residue in quinol binding and in direct deprotonation of the substrate.

We have found that in the acidophilic and chemolithotrophic bacterium *Acidithiobacillus ferrooxidans*, two bc_1 complexes encoded by two different operons were present and that none of them harbored this crucial cyt *b* glutamic acid 272: instead, an apolar proline was present in both cyt *b* sequences (*46*). The presence of an apolar proline or valine was also observed in other organisms (Figure 2). It was then decided to probe the role of E272 in yeast *S. cerevisiae* by site directed mutagenesis using the biolistic method. We replaced E272 by the non-protonatable residues proline and valine naturally present in some organisms. Our biochemical study indicated that E272 in yeast was not irreplaceable and may not be involved in the quinol binding nor as the first cyt *b* amino acid involved in the substrate deprotonation reaction. The selection of the suppressor mutations in this position 272 with polar but not acidic side chains serine and threonine and their study led us to propose that this residue was likely involved in a later step in the proton exit pathway possibly via interaction with water molecules. These results are discussed in the context of the recently different data published on the role of this glutamate residue in the bc_1 complex functioning at the level of the Q_O site catalysis.

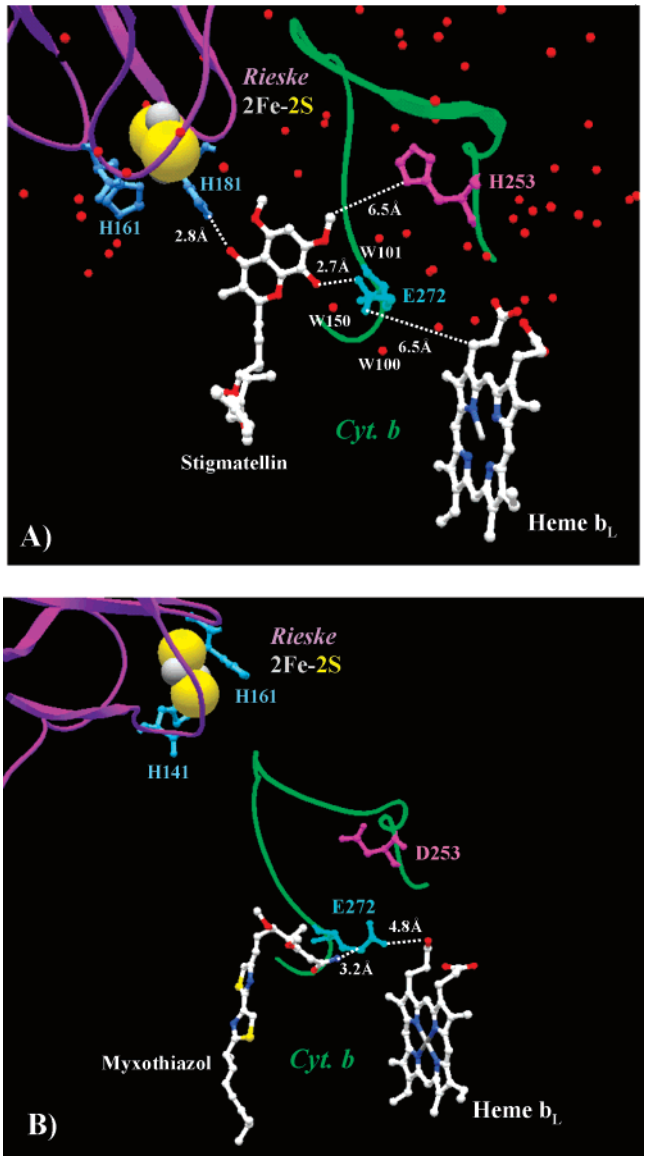

FIGURE 1: Section of cytochrome *b* and Rieske protein in the Q_O site of the yeast bc_1 complex (viewed from the positive side of the inner membrane). Cyt *b* E272 (cyan) is located on the *ef* loop. In panel A, E272 is hydrogen-bonded to stigmatellin, and its side chain is at 6.5 Å from the closest atom of heme b_L, whereas in panel B (in the presence of the inhibitor myxothiazol), the E272 side chain is moved toward heme b_L at 4.8 Å from the heme propionate. H253 is facing E272 in the *ef* loop at 6.5 Å from stigmatellin. Heme b_L and the inhibitors stigmatellin (A) and myxothiazol (B) are shown in CPK colors. The two histidine H161 and H181 (H141 and H161 in the bovine enzyme, panel B) ligands of the [2Fe-2S] cluster (gray and yellow balls) are shown in blue. Water molecules (in panel A) are shown as red dots. For clarity, only the *ef* loop, heme b_L, and the region of the [2Fe-2S] cluster of the ISP are shown. Distances are 2.7, 6.5, and 2.8 Å between cyt *b* E272, H253, ISP H181, and the polar head of the center O inhibitor stigmatellin, respectively. Distance is 3.2 Å between cyt *b* E272 and nearest atom of the center O inhibitor myxothiazol. In the presence of stigmatellin (A), the Rieske [2Fe-2S] cluster is in the proximal position, close to cyt *b* (*23*, *25*, *26*, *42*), whereas in the presence of myxothiazol, the [2Fe-2S] cluster is in the distal position, closer to cyt c_1 (*23*, *25*). The coordinates of the yeast mitochondrial bc_1 complex in the presence of stigmatellin (*26*) were used in panel A (accession no. 1EZV in the Brookhaven Protein Data Bank). The bovine bc_1 complex in the presence of myxothiazol (*43*) is shown in panel B (accession no. 1SQP).

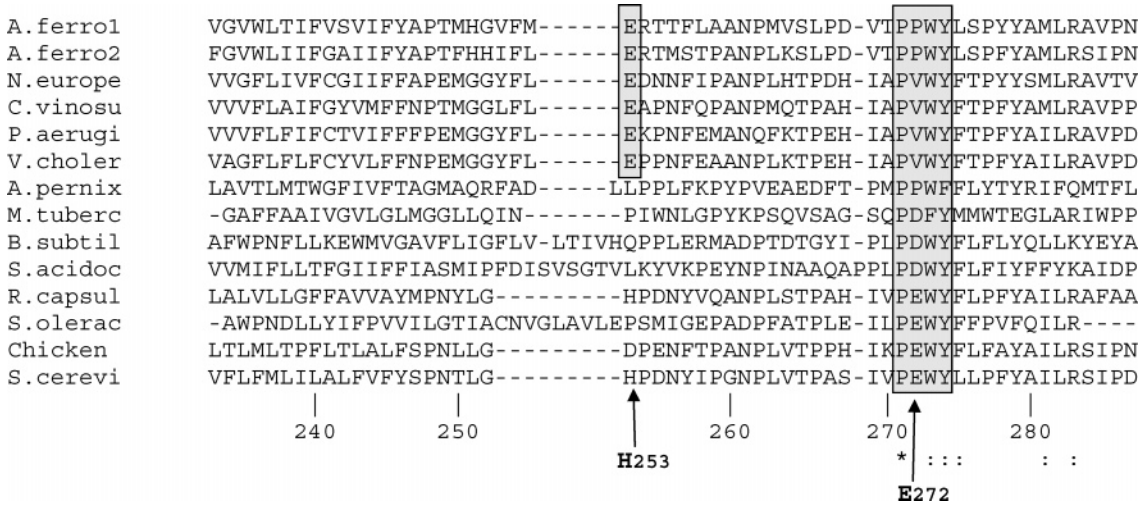

FIGURE 2: Cytochrome *b* sequence alignments of the region encompassing the PEWY motif of the bc/b_6f complexes. The numbers correspond to the yeast *S. cerevisiae* sequence. The asterisk indicates the totally conserved residue proline 271 of the P-E_{272}-W-Y- motif (shaded in gray). Arrows indicate amino acids H253 and E272 discussed in this study. A. ferro1: *Acidithiobacillus ferrooxidans* pet1; A. ferro2: *Acidithiobacillus ferrooxidans* pet2; N. europe: *Nitrosomonas europea*; C. vinosu: *Chromatium vinosum*; P. aerugi: *Pseudomonas aeruginosa*; V. choler: *Vibrio cholerae*; A. pernix: *Aeropyrum pernix*; M. tuberc: *Mycobacterium tuberculosis*; B. subtil: *Bacillus subtilis*; S. acidoc: *Sulfolobus acidocaldarius*; R. capsul: *Rhodobacter capsulatus*; S. olerac: *Spinacia oleracea*; Chicken: *Gallus gallus*; and S. cerevi: *Saccharomyces cerevisiae*. The alignment was performed on the entire cyt *b* genes using the program Clustal W.

MATERIALS AND METHODS

Media, Growth Conditions, in Vivo Phosphorylation Efficiency, and Preparation of Mitochondria. The growth medium contained 2% yeast extract (Difco), 1% bactopeptone (Difco), 0.12% ammonium sulfate, 0.1% glucose, and 2% galactose as the energy source. A total of 1 mL of preculture was used to inoculate toxin flasks containing 500 mL of medium vigorously shaken at 28 °C and harvested 48 h later (beginning of the stationary phase). Growth yield, phosphorylation efficiency, and growth rate were determined as outlined in refs *47* and *48*. Preparation of mitochondria was performed according to the method of Guerin et al. (*49*) with slight modifications (*50*).

Generation of the Mutant Strains. The plasmid pBM5 carrying the WT intronless sequence of the gene *CYTB*, encoding for cyt *b*, was constructed by blunt end cloning of a PCR product of *CYTB* into the pCRscript vector (Stratagene). The mutagenesis was performed using the QuikChange Site-Directed Mutagenesis Kit (Stratagene) according to the manufacturer's recommendations. After verification of the sequence, the plasmids carrying the mutated genes were used for biolistic transformation. The mitochondrial transformation by microprojectile bombardment was adapted from ref *51* and described in refs *52* and *53*.

Isolation and Genetic Analysis of the Revertants. The respiratory growth deficient diploid strain, E272P, generated by biolistic transformation was used to select revertants as follows. The mutant was subcloned. Several subclones were grown in YPD (yeast extract 1%, peptone 2%, and glucose 3%), and then incubated on glycerol respiratory medium (YPG, yeast extract 1%, peptone 2%, and glycerol 3%). Respiratory competent clones appeared after 2 or 3 weeks of incubation. Several independent revertants (each from different subclones) were then analyzed. Their *CYTB* gene was sequenced to identify the secondary changes.

Activities of the Whole Respiratory Chain and of Its Various Segments. All the respiratory activities were carried out on isolated mitochondria. For the whole chain, they were as described in ref *50* in the MR3 buffer (0.65 M sorbitol, 10 mM KH_2PO_4, 2 mM EDTA, 0.1 mM $MgCl_2$, and 0.3% bovine serum albumin, pH 6.5) with a Gilson oxygraph. The various segment activities described next were measured at 25 °C in phosphate buffer (50 mM potassium phosphate and 50 μM EDTA, pH 7.4), using the dual wavelength-stirred reaction cuvette procedure with an Aminco DW2A spectrophotometer (*54*). Complex III, or the DBH_2-cyt *c* reductase activity, was determined by measuring the reduction of cyt *c* (40 μM) at 550 nm using 540 nm as a reference in the presence of KCN (2 mM) with decylubiquinol (50 μM DBH_2) as the electron donor. The I_{50} value for inhibitors is defined as the concentration required to reduce the DBH_2-cyt *c* reductase activity by 50% and is expressed in mol of inhibitor per mol of cyt *b* content for each strain. The relative inhibitor titer I_{50}^r is the ratio between the I_{50} value in a mutant strain and the I_{50} value obtained with the WT strain and indicates the resistance of a strain to the inhibitor in comparison to the WT strain. The pH titrations of the DBH_2-cyt *c* reductase activity were carried out in phosphate buffer (50 mM potassium phosphate and 50 μM EDTA) equilibrated to the required pH value from 5 to 8.7 with the pH incremented in 0.2 unit steps. Complex IV activity (cytochrome oxidase) was measured at 550/540 nm with reduced cyt *c* (50 μM) as the electron donor. The combined activities of segment I + III (NADH-cyt *c* reductase) or II + III (succinate-cyt *c* reductase) were measured by monitoring the reduction of cyt *c* at 550/540 nm with NADH or succinate as the electron donor, in the presence of 2 mM KCN. Extinction coefficients of 6.22, 16, 18, 21.4, and 24 mM^{-1} cm^{-1} were used for the calculation of NADH, DB, cyt $c + c_1$, cyt aa_3, and cyt *b*, respectively.

Spectral Analysis. Mitochondrial membranes were suspended in MR3 buffer, and optical absorption spectra were obtained at 25 °C using a dual wavelength DW2000 SLM-Aminco spectrophotometer as previously described (*50*).

Table 1: Growth Characteristics of the Strains[a]

strains	growth on respiratory substrates (glycerol, EtOH)	doubling time on EtOH (h)	phosphorylation efficiency on EtOH	doubling time on galactose (h)	phosphorylation efficiency on galactose
WT	+	3.6	100	2	100
E272P	−[b]	na	na	2.9	50
E272V	+	4.7	90	2.1	92
E272S	+	4.7	90	2.7	96
E272T	+	4.3	100	2	98

[a] Strains were constructed as described in the Materials and Methods. Growth on respiratory medium (2% glycerol, 2% EtOH) was checked on plates and in liquid medium. The doubling time (growth rate) was measured in liquid media (2% galactose or 2% EtOH). The phosphorylation efficiency (mol of ATP synthesized/mol of substrate consumed) was calculated as in ref *47* and is referred to as growth yield. na: not applicable. [b] Small colonies appeared after 1 week on YPG plates.

Presteady-State Cytochrome Reduction Kinetics by the Center O and Center I Pathways. Cyt *b* reduction kinetics was monitored at 562 nm using 575 nm as a reference with a dual-wavelength SLM-Aminco DW2000 spectrophotometer equipped with a rapidly stirred reaction cuvette in the fast response mode and with the kinetic chopper speed (the lag time of the apparatus was less than 50 ms). NADH (2 mM) was used as the electron donor. Antimycin or myxothiazol were used at saturating levels to observe the center P and center I cyt *b* reduction kinetics, respectively. Cytochrome $c + c_1$ reduction kinetics by the high potential electron transfer pathway was recorded at 551.5/540 nm in the presence of 2 mM KCN.

EPR Spectroscopy. EPR spectra were recorded at 15 K on a Bruker Elexsys X-band spectrometer equipped with an Oxford Instruments liquid helium cryostat and temperature control system. Mitochondrial membranes were suspended in 0.65 M sorbitol, 10 mM Tris-HCl, 2 mM EDTA, and 0.1% bovine serum albumin, pH 6.5.

Molecular Representation. Molecular representation was carried out using the Swiss-PDB Viewer software (*55*). The X-ray coordinates of the yeast mitochondrial bc_1 complex in the presence of the inhibitor stigmatellin (*26*) (accession no. 1EZV in the Brookhaven Protein Data Bank) or the bovine bc_1 complex in the presence of the inhibitor myxothiazol (PDB no. 1SQP, ref *43*) were used to visualize the regions of cyt *b* and ISP described in this study and to calculate the closest distances between selected atoms.

Chemicals. Inhibitors were used in the form of stock ethanolic solutions. Antimycin and decylubiquinone were obtained from Sigma, myxothiazol from Boehringer, and stigmatellin from Fluka. All other chemicals were reagent grade and were purchased from commercial sources.

RESULTS

Conservation of Residue E272, Generation of the E272 Mutants, and Selection and Genetic Characterization of the Suppressors. The yeast mutants harboring the site directed mutations E272P,V in the mitochondrially encoded cyt *b* were generated by the biolistic method (see Materials and Methods). The glutamic acid residue E272 is located in the cyt *b ef* loop (Figure 1), in the so-called PEWY conserved region of the Q_O site. Among these four conserved amino acids, glutamic acid E272 is the least conserved residue (Figure 2): P271 is totally conserved in the cyt *b* sequences analyzed so far (*3*, *56*). W273 and Y274 are more highly conserved than E272, which is replaced by the conservative aspartic acid in *Bacillus subtilis* and *Sulfolobus acidocaldarius* but is also replaced by the apolar residues proline and valine in *Acidithiobacillus ferrooxidans* (operon pet 1 and pet 2, ref *46*), *Nitrosomonas europea*, *Chromatium vinosum*, *Pseudomonas aeruginosa*, *Vibrio cholerae*, *Aeropyrum pernix* (Figure 2), *Bordetella*, *Neisseria* (*3*), and *Rubrivivax gelatinosus* (*57*). E272 is hydrogen-bonded to the inhibitor stigmatellin (Figure 1A), and its side chain is moved toward heme b_L (at 4.8 Å from the heme propionate) in the presence of the inhibitor myxothiazol (Figure 1B). If this residue is crucial for the bc_1 complex functioning, one might expect that this residue should be totally conserved and that mutations of E272 to residues other than acidic amino acids would greatly impede the quinol binding and its deprotonation. We have thus replaced E272 in yeast by the apolar residues proline and valine, which are naturally present in some organisms cited previously. The resulting mutant cells E272V were respiratory growth competent, whereas E272P was unable to grow on respiratory medium. The respiratory growth defect of E272P provided an easy handle to select suppressors. Respiratory competent clones were selected on the respiratory medium, and the heredity of the suppressor mutations was determined. Eleven independent clones were obtained harboring reversions at the same cyt *b* position 272. The sequences of the gene revealed that P272 (codon CCA) was changed into threonine in eight independent clones (one ACA and seven CTA codons) and serine in three independent clones (TCA).

A detailed analysis of the effects of E272P,V mutations and of the reversions E272S,T was then performed. The strains used for the analysis were diploid strains homozygous for the nuclear genes and carry the mitochondrial WT or the mutant E272P,V,T,S cyt *b* (Table 1).

Growth Characteristics. The mutant strain E272P was unable to grow on respiratory medium such as ethanol or glycerol (Table 1) (tiny colonies appeared after 1 week on YPG) and exhibited a lower growth yield (50%) on fermentable substrates such as galactose due to its absence of growth using the respiratory chain. The mutant E272V grew on respiratory substrates with a rate of 4.7 h on ethanol (3.6 h for the WT strain) and exhibited a growth yield of 90−92% on respiratory and fermentable substrates (Table 1). This indicated that E272V did not exhibit any uncoupling in the respiratory chain or lower efficiency in the production of ATP. The phophorylation efficiency of revertants E272S,T was 90−100% of that of the WT in respiratory and fermentable substrates. Their growth rate was a little slower than the WT rate (3.6 h) on respiratory substrate ethanol (4.7 and 4.3 h for E272S and E272T, respectively; see Table 1), which indicated that their respiration level was lower than that of the WT strain.

Table 2: Cytochromes and ISP Contents[a]

strains	cytochrome content $c + c_1$	b	$a + a_3$	[2Fe-2S] cluster content
WT	100	100	100	100
E272P	94	67	82	96
E272V	97	97	103	102
E272S	110	110	110	90
E272T	90	100	110	90

[a] Cytochrome content is expressed as a percentage of the WT. For the WT strain, the contents in dithionite reduced cytochrome $c + c_1$, b, and $a + a_3$ were 0.85, 0.65, and 0.29 nmol/mg of protein, respectively. The [2Fe-2S] cluster content is expressed as a percentage of the WT content and normalized for cyt *b* concentration in each strain: it was determined by the maximum amplitude of the EPR g_y signal in the presence of stigmatellin.

Cytochrome bc_1 Content. Mutant E272P showed a decrease of about 30% in the cyt *b* content, indicating that the presence of two adjacent prolines in the sequence $PP_{272}WY$ slightly affected the cyt *b* content (Table 2). However, this decrease alone could not account for the respiratory growth deficiency. The levels of cyt $c + c_1$ and of cyt $a + a_3$ of the cytochrome oxidase were similar in mutants and WT strains. The level of the ISP was also unaffected in mutants (90−100% of the WT content (Table 2)), showing that mutations in cyt *b* position 272 did not destabilize the ISP.

Respiratory Rates and Activities of the Mitochondrial Complexes. As shown in Table 3, E272P exhibited 9 and 23% of the control NADH and succinate oxygen reductase activities. In the mutant E272V and the revertants E272S,T, these respiratory activities ranged from 36 to 59% of the WT rate, which still allowed the strains to grow well on respiratory substrates. Similar results were obtained for the succinate and NADH-cyt *c* reductase activities. In all the mutants, the decrease in NADH oxygen reductase and NADH-cyt *c* reductase activities as compared to WT was higher than the decrease in succinate oxygen reductase and succinate-cyt *c* reductase activities (Table 3). This is due to the fact that in yeast, the complex II activity is lower than the NADH-Q reductase activity and is the limiting step between succinate and O_2. Therefore, a decreased activity of complex III affects to a greater extent the NADH oxygen reductase and NADH-cyt *c* reductase activities than the succinate oxygen reductase and succinate cyt *c* reductase activities (see refs *54*, *58*, and *59* for a theoretical analysis). Analysis of the bc_1 complex activity in E272P showed that the turnover number was decreased to 18% of the WT value. This corresponded to the threshold (15−20% of bc_1 activity) required for a well-coupled mutant to be able to grow on respiratory substrates. In the mutant E272V and in the revertants E272S,T, the bc_1 complex activity amounted to 30, 36, and 53% of the WT rate, respectively. The specific activity of the cyt *c* oxidase was not modified (Table 3).

Kinetics of Cyt b and Cyt c_1 Reduction. To investigate as to which step was modified in the mutants and suppressor strains in the complex III function (electron transfer from ubiquinol to cyt *c*; see Table 3), we measured the presteady-state kinetics of reduction of both cyt *b* and cyt cc_1 (Figure 3). According to the Q cycle mechanism (*7*−*10*), cyt *b* can be reduced either by the center O pathway (in the presence of the center I inhibitor antimycin, Figure 3B) or by the thermodynamically unfavorable center I pathway (in the presence of the center O inhibitor myxothiazol, Figure 3C). The kinetics provides a global value for the rate of arrival and binding of the substrate to its site and the rate of the electron transfer steps occurring between this binding site and cyt *b* or c_1. The traces presented in Figure 3 followed pseudo-first-order kinetics. Apparent rate constants were calculated from these kinetics. The rate of cyt cc_1 reduction by the high potential pathway (involving the ISP and cyt c_1) in E272P was decreased to about 50% of the WT rate (Figure 3A). In mutant E272V and in revertants E272S,T, the rates ranged from 60 to about 75% of the WT rate. Within the limitations of the experiment (lag time of the apparatus was less than 50 ms), the cyt *b* reduction kinetics through center O appeared to be unaffected in all the strains tested, including E272P (Figure 3B). The cyt *b* reduction kinetics by the reverse electron transfer in the center I pathway (in the presence of the center O inhibitor myxothiazol) was not affected in the mutants E272P,V (Figure 3C); this is in agreement with the locations of the mutations in the Q_O site, on the other side of the membrane.

Quinol and Inhibitor Binding at the Q_O Site. The E272 residue had been postulated to be directly involved in the substrate quinol binding (*42*). In addition, analysis of the available atomic structures showed that the residue was involved in stigmatelin binding (*23*, *25*, *26*). It was thus important to measure the affinity for quinol and for the Q_O site inhibitors stigmatellin and myxothiazol in the four mutated strains E272P,V,T,S. The K_m value for the substrate DBH_2 was obtained by measuring the cyt *c* reductase activity in the presence of varying concentrations of DBH_2 while maintaining cyt *c* at saturating levels. It should be noted that the K_m value is a complex parameter in the bc_1 catalysis involving both quinol oxidation at the Q_O site and quinone reduction at the Q_I site. Results in Table 4 show that all the mutants exhibited very similar K_m values for DBH_2 (values ranged from 3.7 to 4.2 μM and 4 μM for WT). Even in E272P,V lacking a protonated amino acid side chain, the binding of the quinol was not modified. This indicates that

Table 3: Respiratory Rates and Enzymatic Activities of the Different Complexes[a]

strains	NADH-O_2	succinate-O_2	NADH-cyt *c*	succinate-cyt *c*	complex III DBH_2-cyt *c* (T.N.)	complex IV cyt *c* oxidase (T.N.)
WT	100	100	100	100	100	100
E272P	9	23	6	24	18	100
E272V	36	55	37	81	30	106
E272S	41	46	38	95	36	105
E272T	53	59	39	95	53	109

[a] All activities are expressed as percentages of the WT values. With the WT strain, the values obtained were as follows: NADH oxygen reductase, 0.32 μmol of O_2 min^{-1} mg^{-1}; succinate oxygen reductase, 0.22 μmol of O_2 min^{-1} mg^{-1}; NADH cyt *c* reductase, 3.5 μmol of cyt *c* reduced min^{-1} mg^{-1}; succinate cyt *c* reductase, 0.59 μmol of cyt *c* reduced min^{-1} mg^{-1}; complex III (DBH_2 cyt *c* reductase) turnover number (T.N.), 75 s^{-1}; and complex IV (cyt *c* oxidase) turnover number, 110 s^{-1}. Values are based on the average of several experiments.

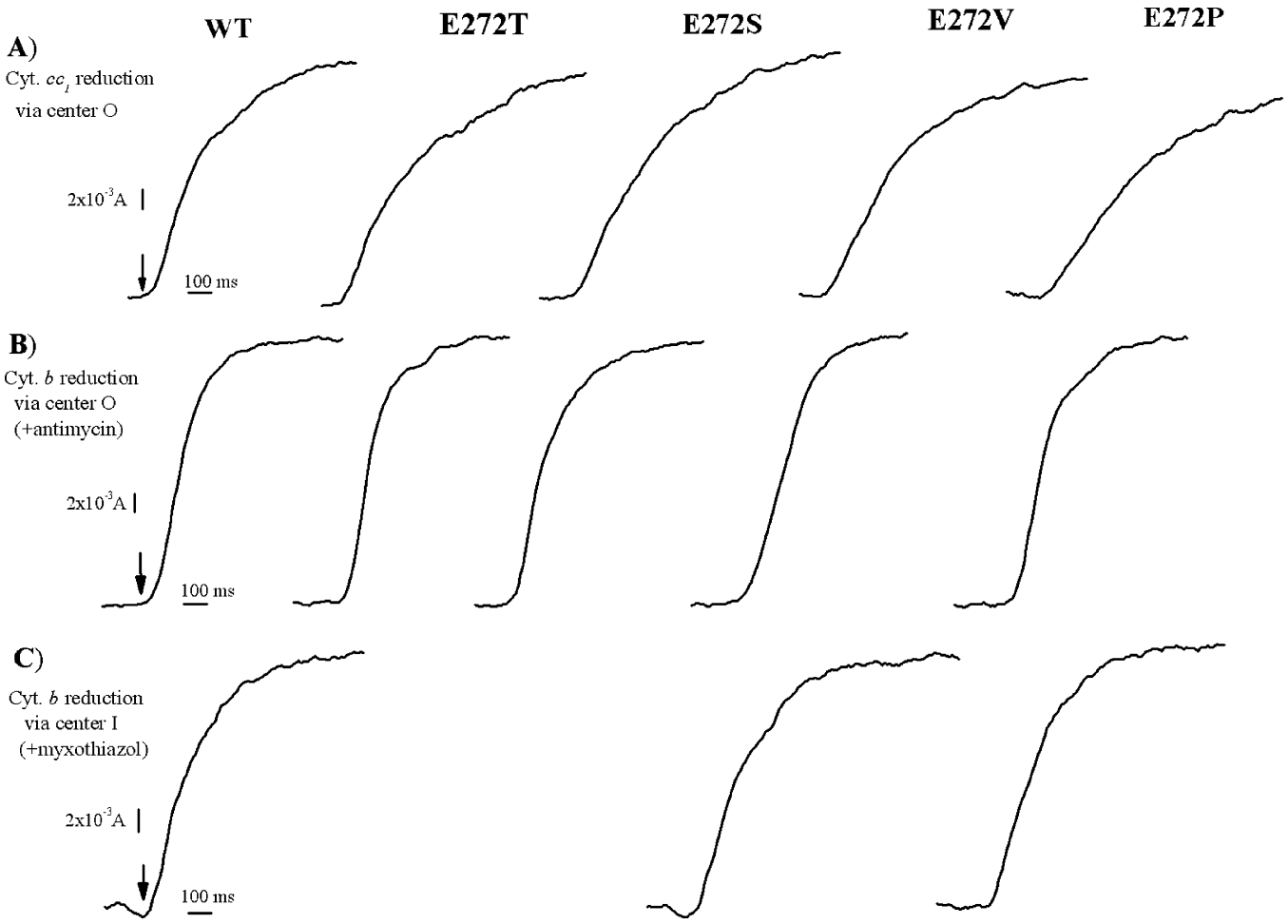

FIGURE 3: Presteady-state kinetics of reduction of the bc_1 complex via the center O and center I pathways. (A) Reduction kinetics of cyt cc_1 via the center O pathway. A mixture of NADH (2 mM) and KCN (2 mM) was used to initiate the cyt reduction (marked by an arrow). Reaction was followed in the dual mode at the wavelength pair 551/540 nm. (B) Reduction kinetics of cyt *b* (562/575 nm) via the center O pathway (in the presence of the center I inhibitor antimycin). (C) Reduction kinetics of cyt *b* via the center I pathway (in the presence of the center O inhibitor myxothiazol). The same final amount of substrate-reducible cyt $c + c_1$ (in panel A) or cyt *b* (in panels B and C) was present in the WT and mutant strains.

E272 does not seem to be a crucial residue for the substrate quinol binding in the Q_O site. As shown in Table 4, the V_m value was, however, decreased in the mutant strains: the lower steady-state turnover was responsible for the decrease in k_{min} (catalytic efficiency, V_m/K_m).

Analysis of the sensitivity to inhibitors showed that none of the mutants exhibited a strong resistance or hypersensitivity for stigmatellin (Figure 4B). The relative inhibitor titer (I_{50}^r) obtained for the mutants ranged between 0.4 and 1.4 (Table 4). Despite the loss of a hydrogen-bond between E272 and stigmatellin in the mutants, the binding of stigmatellin was not drastically perturbed. These results were in contrast to the recent data showing that in the yeast enzyme, different substitutions at position 272 (E272Q,D) induced a resistance to stigmatellin (*44*). The binding of the Q_O site inhibitor myxothiazol, however, was strongly modified in the mutant E272P and to a lesser extent in E272V (Figure 4A). E272P and E272V increased the resistance 2150- and 6-fold, respectively (Table 4). The side chain of E272 is located in proximity to myxothiazol (3.2 Å to the closest atom of the inhibitor (Figure 1B)). The hydrophobic side chains of E272P,V might cause the resistance. Mutants E272S,T with a hydroxyl group and a less bulky side chain than E272P,V did not show any resistance toward myxothiazol (Figure 4A and Table 4).

Q_O Site Occupancy Examined by EPR Spectroscopy. The Q_O site occupancy was monitored using the EPR signal characteristic of the interaction between the ISP [2Fe-2S] cluster and the quinone/quinol bound at the Q_O site. It is well-known that a g_x signal centered at $g = 1.80$ is observed when the Q pool is fully oxidized (E_h around 200 mV) and that this signal shifts to a lower g_x value of around 1.77 when the Q pool is fully reduced (E_h around 0 mV) (*12*, *60*, *61*). When the Q_O site is empty, due to either mutation or extraction of quinone, the value of the g_x signal shifts to a lower value of around 1.76 (*12*). A value of $g_x = 1.78$ is observed when the Q_O site is occupied by the inhibitor stigmatellin (*62*).

The WT sample reduced with ascorbate showed an EPR spectrum with a g_y signal centered at $g = 1.893$ and a g_x trough at $g = 1.80$, characteristic of a Q_O site fully occupied with oxidized quinone (Figure 5A). In all the mutants tested, E272P,V,T,S, the g_x signal was centered at the same value of $g = 1.80$ (with a slightly less pronounced trough for E272S) and was not shifted to a higher magnetic field as is the case in yeast mutants affected in substrate binding (*52*,

Table 4: Catalytic Properties of the bc_1 Complex with the Substrate DBH_2 (V_m, K_m, and k_{min}) and Resistance to Inhibitors Myxothiazol and Stigmatellin[a]

strains	V_m (s^{-1})	K_m DBH_2 (μM)	$k_{min} = V_m/K_m$ (μM^{-1} s^{-1})	I_{50}^r for myxothiazol	I_{50}^r for stigmatellin
WT	61	4	15.3	1	1
E272P	12	3.7	3.2	2150	0.9
E272V	26	4.2	6.2	6.2	1.4
E272S	28	3.9	7.1	0.8	0.4
E272T	42	4.2	10	0.9	0.9

[a] V_m represents the maximum DBH_2 cyt *c* reductase activity (mol of cyt *c* reduced s^{-1}/mol of cyt *b*) measured at 550/540 nm with a dual wavelength spectrophotometer. K_m for DBH_2 was deduced from the titration of the cyt *c* reductase activity with increasing amounts of the substrate DBH_2 and was plotted with a Lineweaver−Burk plot (not shown). k_{min} (V_m/K_m) represents the enzyme catalytic efficiency for the substrate DBH_2. The inhibitor titers I_{50} (concentration of inhibitor required to reduce the DBH_2 cyt *c* reductase activity by 50%; see Figure 4) were 0.65 mol of myxothiazol/mol of cyt *b* and 1 mol of stigmatellin/mol of cyt *b* in the WT strain. The relative inhibitor titer (I_{50}^r) is the ratio of I_{50} obtained with the mutants relative to that in the WT.

53). This indicates that the binding of the quinone was conserved in the mutants despite the absence of E272. When the WT sample was reduced with dithionite (Figure 5B) and the Q pool was fully reduced, the g_x signal was shifted from $g_x = 1.80$ (Q pool oxidized, Figure 5A) to a value of $g_x = 1.78$, thus showing the response of the EPR g_x signal of the [2Fe-2S] cluster to the redox state of the Q pool. All the mutants exhibited the same signal, indicating that they responded well to the redox state of the Q pool. These results were in agreement with the unchanged K_m value for quinol found in mutants (Table 4). Thus, EPR data and the analysis

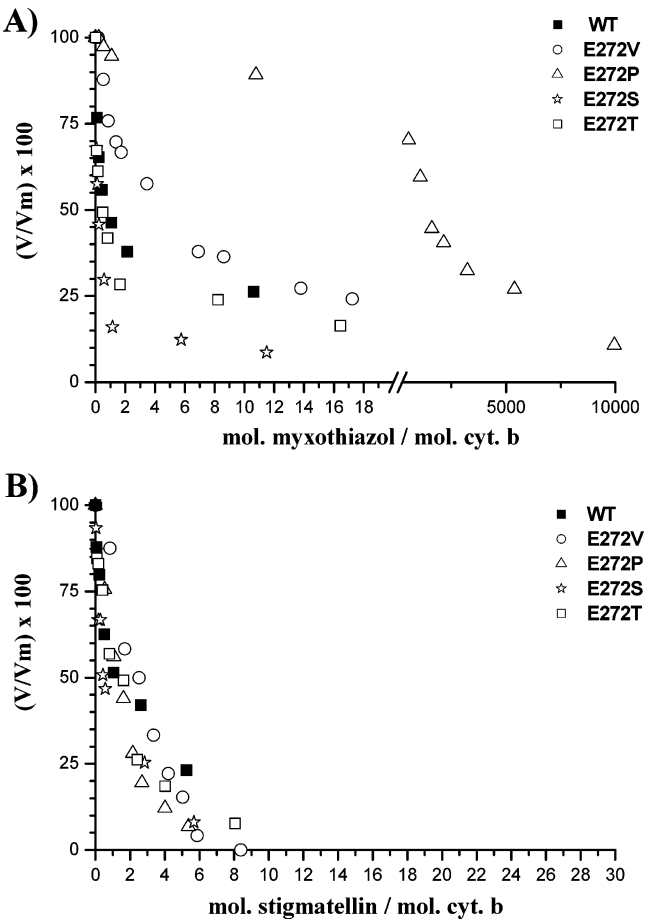

FIGURE 4: Myxothiazol and stigmatellin titration on the DBH2 cyt *c* reductase activity. V_m represents the maximum DBH_2 cyt *c* reductase activity for each strain measured at 25 °C as described in the Materials and Methods. Myxothiazol (A) and stigmatellin (B) were incubated 2 min before the measurement was initiated with DBH_2. Note the break and the different scales present in the *x*-axis in panel A due to the high resistance toward myxothiazol of E272P. See Table 4 for the quantification of the relative inhibitor titers (I_{50}^r).

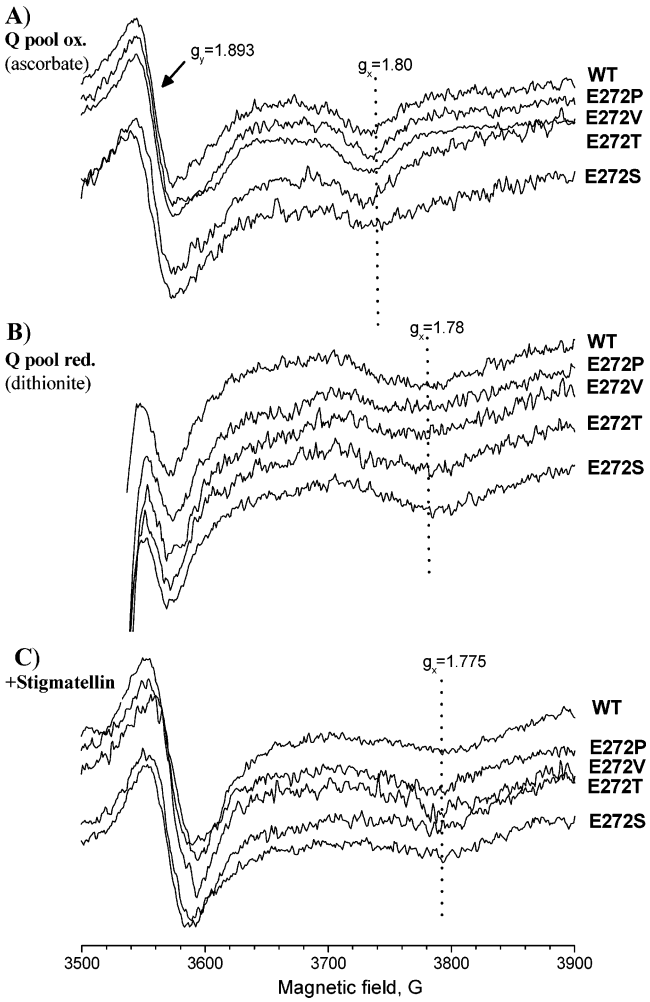

FIGURE 5: Q_O site occupancy probed by EPR spectroscopy of the Rieske protein [2Fe-2S] cluster. EPR spectra were recorded after mitochondrial membranes were reduced (A) with 5 mM ascorbate (Q pool oxidized) or (B) with a few grains of dithionite (Q pool completely reduced) or (C) after the addition of stigmatellin at a final concentration of 10 μM. Arrows and vertical dot lines indicate the *g* values. See Table 2 for the quantification of the ISP in the different strains. Spectra obtained in the presence of dithionite (B) exhibited a lower g_y signal due to a negative contribution of the complex II iron sulfur clusters. EPR conditions were as follows: temperature, 15 K; microwave frequency, 9.42 GHz; microwave power, 6.3 mW; modulation frequency, 100 kHz; and modulation amplitude, 1.6 mT.

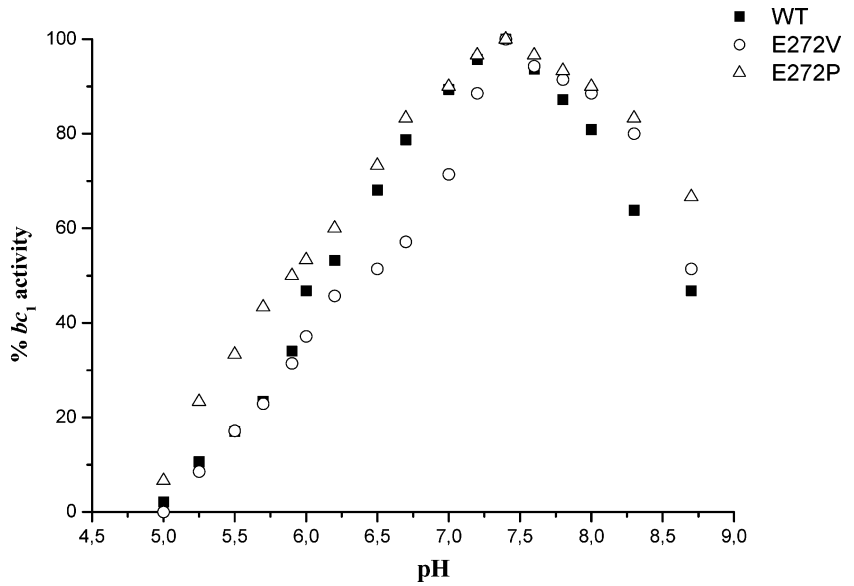

FIGURE 6: pH dependence of the DBH_2 cyt *c* reductase activity. The 100% activity corresponds to 13, 23, and 75 s^{-1} for E272P (△), E272V (○), and WT (■) strains, respectively. Above pH 9, the non-enzymatic rate of cyt *c* reduction is very high and impedes measurements.

of K_m for quinol suggested that position 272 was not crucial for substrate binding even in mutant E272P with the lowest activity and with two adjacent prolines (sequence $PP_{272}WY$).

After the addition of stigmatellin, the ISP [2Fe-2S] cluster was fixed in a position close to cyt *b* (Figure 1A). Mutants and WT exhibited the same g_x trough centered at $g_x = 1.775$ in the presence of stigmatellin (Figure 5C). Thus, EPR data showed that the inhibitor could still bind and that no g_x shift was observed in the mutants, which was in agreement with the inhibitor titration experiments (Figure 4B and Table 4).

pH Dependence of the DBH_2 Cyt c Reductase Activity. E272 had been proposed to be one of the key residues—with ISP H181—involved in the pH dependence of the bc_1 complex activity. If the deprotonated glutamate E272 is the first proton acceptor from quinol on cyt *b*, then the replacement of E272 by a non-protonated group such as proline or valine could modify the pH profile of the bc_1 activity. Figure 6 shows that in the pH range from 5 to 8.7—quinol cyt *c* reductase activity was not measurable outside that pH range—the WT and the two mutants E272P,V with apolar residues exhibited a similar bell-shaped curve, with a maximum activity centered at pH 7.4. The maximal activity was not shifted to higher pH values in the mutants E272P,V, which could have been expected if E272 were crucial as the first proton acceptor from quinol. E272P,V still exhibited a substantial activity at pH < 6, which was in contrast to the results obtained in yeast mutants E272D,Q (*44*). Thus, our results argue against a major role of E272 in the direct binding and deprotonation of the substrate quinol in the Q_O site of the bc_1 complex.

DISCUSSION

For a long time, it was generally considered that the cyt *b* residue E272 in the $PE_{272}WY$ sequence was completely conserved in all the organisms (*56*). A more detailed analysis (refs *3* and *46* and Figure 2 in our study) revealed that this residue is also replaced by the hydrophobic amino acids proline or valine in some organisms. On the basis of the three-dimensional structure of bc_1 in the presence of the inhibitor stigmatellin hydrogen-bonded with E272, Crofts et al. (*42*) proposed that the binding of the quinol in the distal site of the Q_O site directly involved this residue E272, which would be the first proton acceptor in cyt *b* from the substrate quinol. If such a mechanism had been conserved during evolution, this critical residue should be completely conserved or substituted only with protonatable amino acids. On the basis of these observations, we have undertaken the study of mutations of glutamate E272 by the non-protonable hydrophobic residues valine and proline that are naturally present in some organisms (Figure 2). The respiratory growth defect of E272P provided an interesting tool to select the reversions serine and threonine that gave additional information as to the role of this residue E272. Three other possible substitutions from the mutant E272P (codon CCA), in addition to serine and threonine, could have been obtained by a single base change, namely, alanine, glutamine, and arginine. As they were not found in the selection of suppressors, it may be suggested that these substitutions would lead to a deleterious phenotype (absence of respiratory growth) due to their bulkier (Arg and Gln) or hydrophobic (Ala) side chain, which could remove the water molecules in the vicinity of E272 (Figure 1A). All the other amino acid substitutions required two or three base replacements that would be most unlikely. Note that the two residues serine and threonine found in the revertants have polar and smaller side chains than proline and valine. This might allow the water molecules to be hydrogen-bonded to position 272 (see following discussion). Analysis of the growth phenotypes of the different strains shows that whereas the mutant E272P barely grew on respiratory substrates after 1 week, E272V,S,T grew well on respiratory substrates. They exhibited a growth rate slightly slower than WT but the same growth yield on respiratory substrates (Table 1). This showed that despite the absence of glutamate E272, uncoupling did not occur, which could have been caused, for example, by a lower ratio of ejected protons/transferred electrons and/or by higher and wasteful short-circuit reactions resulting in the production of reactive oxygen species. The lower respiratory activity was due to a lower electron transfer rate at the level of the bc_1 complex activity (Table 3). This lower steady-state

DBH2-cyt *c* reductase activity observed in the mutants (between 18 and 53% of the WT rate, Table 3) was not due to an assembly defect. The level of cyt *b* in the mitochondrial membrane of E272P and E272V was 70 and 100% of the WT level (Table 2), and the ISP content normalized for the cyt *b* concentration was also present at nearly WT level in all the stains tested (Table 2). The decreased electron transfer rate was localized at the Q_O site: electron transfer by the high potential pathway involving ISP and cyt c_1 was slowed down in the mutants E272P,V and to lesser extent in revertants E272S,T (Figure 3A). The reduction kinetics of cyt *b* by the center O pathway (Figure 3B) seemed to be less affected than the high potential pathway; however, this may be due to the technical limitations of the experiments: the time scale used in our study was longer than the submillisecond electron transfer rates recently observed by Zhu et al. with an ultrafast freeze-quenching device (*20*). Wenz et al. (*63*) reported recently that E272Q exhibited the same kinetic behavior, namely, slowed down reduction kinetics of cyt c_1, whereas the cyt *b* reduction by the Q_O site was not affected.

Substrate and Inhibitor Binding. By probing the quinol binding in the different strains, we found that in all the mutants studied, even in the more severely affected mutant E272P with only 18% of bc_1 complex activity, the apparent K_m value for ubiquinol did not differ from that of the WT strain (around 4 μM, Table 4). EPR experiments were performed to probe the g_x signal of the ISP, known to be sensitive to quinol occupancy and to the redox state of the quinone pool. Results showed that all the mutants exhibited an EPR g_x signal in the presence of quinone ($g_x = 1.80$) similar to the WT and that the signal responded well to the redox state of the Q pool as shown by its displacement toward a higher magnetic field when the Q pool was reduced ($g_x = 1.78$). In mutants with a quinol binding deficiency, the quinone g_x signal at $g = 1.8$ is usually broadened and upfield shifted to around $g = 1.7$, which was not the case in E272P,V,S,T. These results thus differed from the data previously obtained with the yeast mutants E272Q,D (*44*), where a lower K_m (higher affinity) for decylubiquinol was observed in the mutants. In addition, the EPR spectra of E272D showed different g_z and g_x signals in the presence of dithionite, which would indicate perturbed quinol binding. Our data, on the other hand, are in agreement with the results published recently in ref *45*. These authors showed that in all the *R. capsulatus* E295V,Q,F,A,K,H mutants (position equivalent to E272 in yeast), the EPR signals were not modified in the presence of quinone and quinol. Similar results were obtained for the EPR spectra in the presence of the inhibitor stigmatellin, where both in our study and in ref *45* the EPR g_x was not modified in the mutants. Data in Figure 4 and Table 4 showed that mutants E272P,V,T,S did not exhibit a strong resistance or hypersensitivity toward stigmatellin despite its close interaction with the side chain of E272. The loss of the hydrogen-bond between stigmatellin and the side chain of the residue in position 272 in mutants E272P,V did not modify the inhibitor binding strength. It is possible that the hydrogen-bond of the polar head of stigmatellin with E272 could play a minor role in its affinity for the Q_O site, whereas interactions between stigmatellin hydrophobic tail and amino acids in a deeper region of cyt *b* such as F129 and I147 (shown to be involved in stigmatellin resistance; see ref *64*) would be the major stabilization reactions.

We found that mutations E272P,V with hydrophobic residues decreased the sensitivity of the enzyme toward myxothiazol, another Q_O site inhibitor bound in the proximal site (Figure 1B), by 2000- and 6-fold, respectively (Figure 4A and Table 4). The distance between E272 backbone amino group and myxothiazol is 3.1 Å and between the E272 side chain and the amino group on the polar head of myxothiazol is 3.3 Å (Figure 2B): this short distance could explain the effects of the mutations on the inhibitor binding. In the mutant E272P, the presence of a double kink introduced by the two consecutive prolines in the $PP_{272}WY$ sequence most likely induces a perturbation of the local structure of cyt *b* and that may explain the strong myxothiazol resistance and the lowest bc_1 complex activity observed in this mutant, although the quinol binding was not modified. Note that revertants E272T,S are not resistant toward myxothiazol and have a shorter and polar side chain in position 272 in comparison to resistant mutants E272P,V.

pH Dependence of the bc_1 Activity. Wenz et al. (*44*) reported an altered pH dependence of the bc_1 activity, especially at low pH values, in yeast mutants E272Q,D. The authors suggested that the observation could be explained by the loss of a group with a pK_a value of about 6.2. By contrast, results obtained in *R. capsulatus* did not reveal any effects of E272 mutations on the E_m/pH plots and on the pH profile of the kinetics of electron transfer. These authors ruled out the involvement of E272 in a strong electron−proton coupling in the Q_O site (*45*). Our study showed no significant differences between WT and mutants E272P,V in the pH dependence of the steady-state bc_1 complex activity. A loss of activity was not observed at low pH values (Figure 6), even when E272 was replaced by the hydrophobic residues P and V, which induced a more severe decrease of the steady-state bc_1 complex activity.

Altogether, our results did not favor the involvement of E272 as a crucial residue in direct binding of the substrate quinol and as the first proton acceptor from quinol in cyt *b*. Isolation of the revertants from E272P yielded important additional information about the role of E272. The bc_1 activity in reverants E272T,S was higher than in mutants E272P,V (Table 3). Serine and threonine were not able to directly deprotonate quinol. However, their hydroxyl group can be hydrogen-bonded to water molecules present in the Q_O site. In the yeast stigmatellin-bound cyt *b* structure (*26*), E272 is located 2.6−2.8 Å from three water molecules, H_2O 100, 101, and 150 (Figure 1A). Palsdottir et al. (*18*) reported that contrary to stigmatellin, the Q_O site inhibitor HHDBT was not hydrogen-bonded to the side chain of E272, and this latter was rotated toward heme b_L propionate A. These authors proposed that HHDBT mimicked an intermediate step of ubiquinol oxidation after its deprotonation. Note that the position of glutamate 272 of the stigmatellin-bound structure was occupied by a water molecule hydrogen-bonded to HHDBT and to the backbone nitrogen atom of E272. Recently, Giachini et al. (*65*) proposed that in the Q_O site of avian and bovine bc_1 complexes, H121, H268, K270, and D253 would be involved in the binding of Zn^{2+} and that in the *R. capsulatus* bc_1 complex, E295 (equivalent to E272 in yeast) would be a Zn^{2+} ligand, located at the entrance of the putative proton release pathway. One or several of the water

molecules hydrogen-bonded to E272 may be crucial for proton conduction. They may be involved in forming a proton wire for the exit of protons after a quinol deprotonation event. In the case of the mutants E272P,V with a hydrophobic side chain, hydrogen-bonding between residue 272 and these water molecules would be lost and the proton exit pathway altered. In revertants E272S,T that can form hydrogen-bonds with these water molecules, the exit route would be partially restored, which might explain the higher bc_1 activity.

Thus, we suggest that E272 would not be a quinol binding residue but would be involved in a water molecule hydrogen-bond network that would be needed in the proton exit pathway. E272 would not be the first proton acceptor from quinol in cyt *b* but would be involved in a later step. This is in agreement with results showing that quinol binding was not affected in mutants. The unaltered pH profile of bc_1 activity in mutants E272P,V suggests that E272 would not be the only or the main player in water molecule exchange. It would not be the limiting step in the coupled electron/proton transfer at the Q_O site since its replacement by other amino acids still permitted quinol oxidation, although to a slower rate. This points out the resilience of the Q_O site as described by Osyczka et al. (*45*). The robustness of the mechanism was also observed in the reaction center, where different residues and water molecules can take over the task of proton transfer in some mutants (*66*). It remains to be clarified as to whether only one or several residues are involved in quinol binding and in its direct deprotonation event on cyt *b*. Experimental data point toward several residues participating in the quinol binding as several residues affected the quinol binding in the Q_O site as judged by altered K_m values or by a shifted EPR signal. These residues involved in the substrate binding are F129 (F144 in *R. capsulatus*, ref *61*), G131 (*67*) (G146 in *R. capsulatus*, ref *68*), G143 (G158 in *R. capsulatus*, ref *69*), A144 (*53*), T148 (T163 in *R. capsulatus*, ref *70*), and Y279 (*52*, *63*). They are located in cyt *b* at the end of transmembrane helix C (F129 and G131), in the cd_1 helix (G143, A144, and T148), and at the end of the *ef* loop (Y279).

In evolutionary terms, it may be advantageous to separate amino acids directly involved in substrate quinol binding from those involved in its deprotonation. In the case of the occurrence of point mutations, this would prevent the complete abolition of enzyme activity: it would allow a partial deprotonation rate without adversely lowering the efficacy of quinol binding at the QO site or vice-versa—a partial quinol binding without lowering the efficiency of the deprotonation event. An alternative hypothesis, which could partially reconcile the different suggestions as to the role of E272 (refs *44* and *45* and our study), is that the possible hydrogen-bond between deprotonated cyt *b* E272 and quinol would not be strong enough to stabilize the quinol, which would explain the unchanged binding of the quinone/quinol in the E272 mutants analyzed in our study and in ref *45*. The low affinity (K_m value in the micromolar range) for the substrate quinol would be due to hydrophobic interactions between amino acids and hydrophobic isoprenoid tail of the quinol, rather than to the hydrogen-bond interactions between the polar head of the quinol and the deprotonated cyt *b* E272 and ISP H181. In this case, mutations of E272 would not impair the quinol/quinone binding since it would be mainly due to other residues in a more hydrophobic region of cyt *b*. But mutations would impair partially the deprotonation event and consequently the electron transfer step at the Q_O site. The hydrophilic head of quinol close to the surface of the Q_O site may be more mobile than the hydrophobic tail in the deeper region of cyt *b*: in the absence of E272, deprotonation of quinol (and subsequent electron transfer) may be performed by other deprotonated residues such as H253 (discussed next). The possible effect of E272 on the pH dependence would be masked by other protonic residues and/or water molecules present in the proton exit channel-(s), which would all participate in the pH behavior of the catalysis, in addition to ISP His181, which is critical for the pH dependence of quinol oxidation on the Q_O site.

It is noteworthy that organisms that do not have a glutamic acid at position 272 contain a conserved glutamate residue at the position corresponding to H253 in yeast (Figure 2) (*46*). In *A. pernix*, the protonable residue asparatate is present two residues upstream (Figure 2). In these species, several additional residues were inserted in the *ef* loop that may affect the glutamate 253 positioning, and this residue could be an alternative proton acceptor (*46*). The H253 residue found in yeast is not completely conserved (Figure 2 and refs *3* and *56*); thus, it is unlikely to be essential for the deprotonation of the quinol in organisms that contain E272. However, in organisms without a glutamate at position 272, E253 might be important to deprotonate the quinol. This residue H253 is located at 6.5 Å from the closest atom of stigmatellin in the cyt *b* distal site (Figure 1A). D253 (present in the bovine bc_1 structure) is located at 9 Å from the proximal site inhibitor myxothiazol (Figure 1B). Palsdottir et al. (*18*) proposed that H253 was hydrogen-bonded with E272 in the proton exit pathway. Studies are in progress to elucidate the role of this residue in the functioning of the bc_1 complex, but preliminary data showed that like E272, H253 is not an irreplaceable residue (unpublished results). Several residues on the proton exit pathway might have to be mutated concomitantly to observe more drastic phenotypes and to completely disrupt the proton conduction by water molecules and protonated residues in the Q_O site.

ACKNOWLEDGMENT

Nick Fisher and Alain Dolla are thanked for help with manuscript preparation.

REFERENCES

1. Brandt, U., and Trumpower, B. L. (1994) The protonmotive Q cycle in mitochondria and bacteria, *Crit. Rev. Biochem. Mol. Biol. 29*, 165−197.
2. Gray, K. A., and Daldal, F. (1995) Mutational Studies of the Cytochrome bc_1 Complexes, in *Anoxygenic Photosynthetic Bacteria* (Blankenship, R. E., Madigan, M. T., and Bauer, C., Eds.) pp 747−774, Kluwer Academic Publishers, Dordrecht, The Netherlands.
3. Berry, E. A., Guergova-Kuras, M., Huang, L. S., and Crofts, A. R. (2000) Structure and function of cytochrome *bc* complexes, *Annu. Rev. Biochem. 69*, 1005−1075.
4. Crofts, A. R. (2004) The cytochrome bc_1 complex: Function in the context of structure, *Annu. Rev. Physiol. 66*, 689−733.
5. Cramer, W. A., Soriano, G. M., Ponomarev, M., Huang, D., Zhang, H., Martinez, S. E., and Smith, J. L. (1996) Some new structural aspects and old controversies concerning the cytochrome b_6f complex of oxygenic photosynthesis, *Annu. Rev. Plant Physiol. Plant Mol. Biol. 47*, 477−508.

6. Cramer, W. A., Zhang, H., Yan, J., Kurisu, G., and Smith, J. L. (2006) Transmembrane traffic in the cytochrome b_6f complex, *Annu. Rev. Biochem. 75*, 769−790.
7. Mitchell, P. (1975) The protonmotive Q cycle: A general formulation, *FEBS Lett. 59*, 137−139.
8. Mitchell, P. (1976) Possible molecular mechanisms of the protonmotive function of cytochrome systems, *J. Theor. Biol. 62*, 327−367.
9. Crofts, A. R., Meinhardt, S. W., Jones, K. R., and Snozzi, M. (1983) The role of the quinone pool in the cyclic electron-transfer chain of *Rhodopseudomonas sphaeroides.* A modified Q-cycle mechanism, *Biochim. Biophys. Acta 723*, 202−218.
10. Trumpower, B. L. (1990) The protonmotive Q cycle. Energy transduction by coupling of proton translocation to electron transfer by the cytochrome bc_1 complex, *J. Biol. Chem. 265*, 11409−11412.
11. Trumpower, B. L. (1976) Evidence for a protonmotive Q cycle mechanism of electron transfer through the cytochrome bc_1 complex, *Biochem. Biophys. Res. Commun. 70*, 73−80.
12. Ding, H., Robertson, D. E., Daldal, F., and Dutton, P. L. (1992) Cytochrome bc_1 complex [2Fe-2S] cluster and its interaction with ubiquinone and ubihydroquinone at the Q_O site: A double-occupancy Q_O site model, *Biochemistry 31*, 3144−3158.
13. Brandt, U. (1996) Bifurcated ubihydroquinone oxidation in the cytochrome bc_1 complex by proton-gated charge transfer, *FEBS Lett. 387*, 1−6.
14. Link, T. A. (1997) The role of the Rieske iron sulfur protein in the hydroquinone oxidation Q_P site of the cytochrome bc_1 complex. The proton-gated affinity change mechanism. *FEBS Lett. 412*, 257−264.
15. Junemann, S., Heathcote, P., and Rich, P. R. (1998) On the mechanism of quinol oxidation in the bc_1 complex, *J. Biol. Chem. 273*, 21603−21607.
16. Crofts, A. R., Guergova-Kuras, M., Huang, L., Kuras, R., Zhang, Z., and Berry, E. A. (1999) Mechanism of ubiquinol oxidation by the bc_1 complex: Role of the iron sulfur protein and its mobility, *Biochemistry 38*, 15791−15806.
17. Snyder, C. H., Gutierrez-Cirlos, E. B., and Trumpower, B. L. (2000) Evidence for a concerted mechanism of ubiquinol oxidation by the cytochrome bc_1 complex, *J. Biol. Chem. 275*, 13535−13541.
18. Palsdottir, H., Lojero, C. G., Trumpower, B. L., and Hunte, C. (2003) Structure of the yeast cytochrome bc_1 complex with a hydroxyquinone anion Q_O site inhibitor bound, *J. Biol. Chem. 278*, 31303−31311.
19. Cape, J. L., Bowman, M. K., and Kramer, D. M. (2007) A semiquinone intermediate generated at the Q_O site of the cytochrome bc_1 complex: Importance for the Q-cycle and superoxide production, *Proc. Natl. Acad. Sci. U.S.A. 104*, 7887−7892.
20. Zhu, J., Egawa, T., Yeh, S. R., Yu, L., and Yu, C. A. (2007) Simultaneous reduction of iron-sulfur protein and cytochrome b_L during ubiquinol oxidation in cytochrome bc_1 complex, *Proc. Natl. Acad. Sci. U.S.A. 104*, 4864−4869.
21. Trumpower, B. L. (1990) Cytochrome bc_1 complexes of microorganisms, *Microbiol. Rev. 54*, 101−129.
22. Xia, D., Yu, C. A., Kim, H., Xia, J. Z., Kachurin, A. M., Zhang, L., Yu, L., and Deisenhofer, J. (1997) Crystal structure of the cytochrome bc_1 complex from bovine heart mitochondria, *Science (Washington, DC, U.S.) 277*, 60−66.
23. Zhang, Z., Huang, L., Shulmeister, V. M., Chi, Y. I., Kim, K. K., Hung, L. W., Crofts, A. R., Berry, E. A., and Kim, S. H. (1998) Electron transfer by domain movement in cytochrome bc_1, *Nature (London, U.K.) 392*, 677−684.
24. Iwata, S., Lee, J. W., Okada, K., Lee, J. K., Iwata, M., Rasmussen, B., Link, T. A., Ramaswamy, S., and Jap, B. K. (1998) Complete structure of the 11-subunit bovine mitochondrial cytochrome bc_1 complex, *Science (Washington, DC, U.S.) 281*, 64−71.
25. Kim, H., Xia, D., Yu, C. A., Xia, J. Z., Kachurin, A. M., Zhang, L., Yu, L., and Deisenhofer, J. (1998) Inhibitor binding changes domain mobility in the iron-sulfur protein of the mitochondrial bc_1 complex from bovine heart, *Proc. Natl. Acad. Sci. U.S.A. 95*, 8026−8033.
26. Hunte, C., Koepke, J., Lange, C., Robmanith, T., and Michel, H. (2000) Structure at 2.3 Å resolution of the cytochrome bc_1 complex from the yeast *Saccharomyces cerevisiae* co-crystallized with an antibody Fv fragment, *Structure 8*, 669−684.
27. Kurisu, G., Zhang, H., Smith, J. L., and Cramer, W. A. (2003) Structure of the cytochrome b_6f complex of oxygenic photosynthesis: Tuning the cavity, *Science (Washington, DC, U.S.) 302*, 1009−1014.
28. Stroebel, D., Choquet, Y., Popot, J. L., and Picot, D. (2003) An atypical haem in the cytochrome b_6f complex, *Nature (London, U.K.) 426*, 413−418.
29. Berry, E. A., Huang, L. S., Saechao, L. K., Pon, N. G., Valkova-Valchanova, M., and Daldal, F. (2004) X-Ray structure of *Rhodobacter capsulatus* cytochrome bc_1: Comparison with its mitochondrial and chloroplast counterparts, *Photosynth. Res. 81*, 251−275.
30. Brasseur, G., Sled, V., Liebl, U., Ohnishi, T., and Daldal, F. (1997) The amino-terminal portion of the Rieske iron-sulfur protein contributes to the ubihydroquinone oxidation site catalysis of the *Rhodobacter capsulatus* bc_1 complex, *Biochemistry 36*, 11685−11696.
31. Tian, H., Yu, L., Mather, M. W., and Yu, C. A. (1998) Flexibility of the neck region of the Rieske iron-sulfur protein is functionally important in the cytochrome bc_1 complex, *J. Biol. Chem. 273*, 27953−27959.
32. Tian, H., White, S., Yu, L., and Yu, C. A. (1999) Evidence for the head domain movement of the Rieske iron-sulfur protein in electron transfer reaction of the cytochrome bc_1 complex, *J. Biol. Chem. 274*, 7146−7152.
33. Nett, J. H., Hunte, C., and Trumpower, B. L. (2000) Changes to the length of the flexible linker region of the Rieske protein impair the interaction of ubiquinol with the cytochrome bc_1 complex, *Eur. J. Biochem. 267*, 5777−5782.
34. Darrouzet, E., Valkova-Valchanova, M., and Daldal, F. (2000) Probing the role of the Fe-S subunit hinge region during Q_O site catalysis in the *Rhodobacter capsulatus* bc_1 complex, *Biochemistry 39*, 15475−15483.
35. Obungu, V. H., Wang, Y., Amyot, S. M., Gocke, C. B., and Beattie, D. S. (2000) Mutations in the tether region of the iron-sulfur protein affect the activity and assembly of the cytochrome bc_1 complex of yeast mitochondria, *Biochim. Biophys. Acta 1457*, 36−44.
36. Darrouzet, E., Valkova-Valchanova, M., Moser, C. C., Dutton, P. L., and Daldal, F. (2000) Uncovering the [2Fe-2S] domain movement in cytochrome bc_1 and its implications for energy conversion, *Proc. Natl. Acad. Sci. U.S.A. 97*, 4567−4572.
37. Brugna, M., Rodgers, S., Schricker, A., Montoya, G., Kazmeier, M., Nitschke, W., and Sinning, I. (2000) A spectroscopic method for observing the domain movement of the Rieske iron-sulfur protein, *Proc. Natl. Acad. Sci. U.S.A. 97*, 2069−2074.
38. Darrouzet, E., Moser, C. C., Dutton, P. L., and Daldal, F. (2001) Large scale domain movement in cytochrome bc_1: A new device for electron transfer in proteins, *Trends Biochem. Sci. 26*, 445−451.
39. Crofts, A., Hacker, B., Barquera, B., Yun, C. H., and Gennis, R. (1992) Structure and function of the *bc*-complex of *Rhodobacter sphaeroides*, *Biochim. Biophys. Acta 1101*, 162−165.
40. Crofts, A. R., Barquera, B., Bechmann, G., Guergova, M., Salcedo-Hernandez, R., Hacker, B., Hong, S., and Gennis, R. B. (1995) Structure and Function in the bc_1 Complex of *Rhodobacter sphaeroides*, in *Photosynthesis: From Light to Biosphere* (Mathis, P., Ed.) Vol. II, pp 493−500, Kluwer Academic Publishers, Dordrecht, The Netherlands.
41. Zito, F., Finazzi, G., Joliot, P., and Wollman, F. A. (1998) Glu78, from the conserved PEWY sequence of subunit IV, has a key function in cytochrome b_6f turnover, *Biochemistry 37*, 10395−10403.
42. Crofts, A. R., Hong, S., Ugulava, N., Barquera, B., Gennis, R., Guergova-Kuras, M., and Berry, E. A. (1999) Pathways for proton release during ubihydroquinone oxidation by the bc_1 complex, *Proc. Natl. Acad. Sci. U.S.A. 96*, 10021−10026.
43. Esser, L., Quinn, B., Li, Y. F., Zhang, M., Elberry, M., Yu, L., Yu, C. A., and Xia, D. (2004) Crystallographic studies of quinol oxidation site inhibitors: A modified classification of inhibitors for the cytochrome bc_1 complex, *J. Mol. Biol. 341*, 281−302.
44. Wenz, T., Hellwig, P., MacMillan, F., Meunier, B., and Hunte, C. (2006) Probing the role of E272 in quinol oxidation of mitochondrial complex III, *Biochemistry 45*, 9042−9052.
45. Osyczka, A., Zhang, H., Mathe, C., Rich, P. R., Moser, C. C., and Dutton, P. L. (2006) Role of the PEWY glutamate in hydroquinone-quinone oxidation-reduction catalysis in the Q_O site of cytochrome bc_1, *Biochemistry 45*, 10492−10503.

46. Brasseur, G., Bruscella, P., Bonnefoy, V., and Lemesle-Meunier, D. (2002) The bc_1 complex of the iron-grown acidophilic chemolithotrophic bacterium *Acidithiobacillus ferrooxidans* functions in the reverse but not in the forward direction. Is there a second bc_1 complex? *Biochim. Biophys. Acta 1555*, 37−43.
47. Chevillotte-Brivet, P., and Meunier-Lemesle, D. (1980) Cytochrome *b*-565 in *Saccharomyces cerevisiae*: Use of mutants in the *cob*-box region of mitochondrial DNA to study the functional role of this spectral species of cytochrome *b*. 2. Relationship between energetic data and cytochrome *b*-565 content, *Eur. J. Biochem. 111*, 161−169.
48. Coppee, J. Y., Brasseur, G., Brivet-Chevillotte, P., and Colson, A. M. (1994) Non-native intragenic reversions selected from *Saccharomyces cerevisiae* cytochrome *b*-deficient mutants. Structural and functional features of the catalytic center N domain, *J. Biol. Chem. 269*, 4221−4226.
49. Guerin, B., Labbe, P., and Somlo, M. (1979) Preparation of yeast mitochondria (*Saccharomyces cerevisiae*) with good P/O and respiratory control ratios, *Methods Enzymol. 55*, 149−159.
50. Meunier-Lemesle, D., Chevillotte-Brivet, P., and Pajot, P. (1980) Cytochrome *b*-565 in *Saccharomyces cerevisiae*: Use of mutants in the *cob*-box region of mitochondrial DNA to study the functional role of this spectral species of cytochrome *b*. 1. Measurements of cytochromes *b*-562 and *b*-565 and selection of revertants devoid of cytochrome *b*-565, *Eur. J. Biochem. 111*, 151−159.
51. Bonnefoy, N., and Fox, T. D. (2001) Genetic transformation of *Saccharomyces cerevisiae* mitochondria, *Methods Cell Biol. 65*, 381−396.
52. Fisher, N., Castleden, C. K., Bourges, I., Brasseur, G., Dujardin, G., and Meunier, B. (2004) Disease-related mutations in cytochrome *b* studied in yeast, *J. Biol. Chem. 279*, 12951−12958.
53. Brasseur, G., Lemesle-Meunier, D., Reinaud, F., and Meunier, B. (2004) Q_O site deficiency can be compensated by extragenic mutations in the hinge region of the Rieske protein in the bc_1 complex of *Saccharomyces cerevisiae*, *J. Biol. Chem. 279*, 24203−24211.
54. Brasseur, G., Coppée, J. Y., Colson, A. M., and Brivet-Chevillotte, P. (1995) Structure−function relationships of the mitochondrial bc_1 complex in temperature-sensitive mutants of the cytochrome *b* gene, impaired in the catalytic center N, *J. Biol. Chem. 270*, 29356−29364.
55. Guex, N., and Peitsch, M. C. (1997) SWISS-MODEL and the Swiss-PdbViewer: An environment for comparative protein modeling, *Electrophoresis 18*, 2714−2723.
56. Degli-Esposti, M., De Vries, S., Crimi, M., Ghelli, A., Patarnello, T., and Meyer, A. (1993) Mitochondrial cytochrome *b*: Evolution and structure of the protein, *Biochim. Biophys. Acta 1143*, 243−271.
57. Ouchane, S., Agalidis, I., and Astier, C. (2002) Natural resistance to inhibitors of the ubiquinol cytochrome *c* oxidoreductase of *Rubrivivax gelatinosus*: Sequence and functional analysis of the cytochrome bc_1 complex, *J. Bacteriol. 184*, 3815−3822.
58. Kröger, A., and Klingenberg, M. (1973) The kinetics of the redox reactions of ubiquinone related to the electron-transport activity in the respiratory chain, *Eur. J. Biochem. 34*, 358−368.
59. Meunier, D., and Chevillotte-Brivet, P. (1977) Effect of antimycin A on succinate oxidase activity in potato tuber mitochondria and the behavior of cytochromes *b*, *J. Theor. Biol. 64*, 137−163.
60. Matsuura, K., Bowyer, J. R., Ohnishi, T., and Dutton, P. L. (1983) Inhibition of electron transfer by 3-alkyl-2-hydroxy-1,4-naphthoquinones in the ubiquinol-cytochrome *c* oxidoreductases of *Rhodopseudomonas sphaeroides* and mammalian mitochondria. Interaction with a ubiquinone-binding site and the Rieske iron-sulfur cluster, *J. Biol. Chem. 258*, 1571−1579.
61. Ding, H., Daldal, F., and Dutton, P. L. (1995) Ubiquinone pair in the Q_O site central to the primary energy conversion reactions of cytochrome bc_1 complex, *Biochemistry 34*, 15997−16003.
62. von Jagow, G., and Ohnishi, T. (1985) The chromone inhibitor stigmatellin binding to the ubiquinol oxidation center at the C-side of the mitochondrial membrane, *FEBS Lett. 185*, 311−315.
63. Wenz, T., Covian, R., Hellwig, P., Macmillan, F., Meunier, B., Trumpower, B. L., and Hunte, C. (2007) Mutational analysis of cytochrome *b* at the ubiquinol oxidation site of yeast complex III, *J. Biol. Chem. 282*, 3977−3988.
64. Brasseur, G., Saribas, A. S., and Daldal, F. (1996) A compilation of mutations located in the cytochrome *b* subunit of the bacterial and mitochondrial bc_1 complex, *Biochim. Biophys. Acta 1275*, 61−69.
65. Giachini, L., Francia, F., Veronesi, G., Lee, D. W., Daldal, F., Huang, L. S., Berry, E. A., Cocco, T., Papa, S., Boscherini, F., and Venturoli, G. (2007) X-ray absorption studies of Zn^{2+} binding sites in bacterial, avian, and bovine cytochrome bc_1 complexes, *Biophys. J. 93*, 2934−2951.
66. Paddock, M. L., Feher, G., and Okamura, M. Y. (2003) Proton transfer pathways and mechanism in bacterial reaction centers, *FEBS Lett. 555*, 45−50.
67. Brasseur, G., Di Rago, J. P., Slonimski, P. P., and Lemesle-Meunier, D. (2001) Analysis of suppressor mutation reveals long distance interactions in the bc_1 complex of *Saccharomyces cerevisiae*, *Biochim. Biophys. Acta 1506*, 89−102.
68. Saribas, A. S., Ding, H., Dutton, P. L., and Daldal, F. (1997) Substitutions at position 146 of cytochrome *b* affect drastically the properties of heme b_L and the Q_O site of *Rhodobacter capsulatus* cytochrome bc_1 complex, *Biochim. Biophys. Acta 1319*, 99−108.
69. Robertson, D. E., Daldal, F., and Dutton, P. L. (1990) Mutants of ubiquinol-cytochrome c_2 oxidoreductase resistant to Q_O site inhibitors: Consequences for ubiquinone and ubiquinol affinity and catalysis, *Biochemistry 29*, 11249−11260.
70. Ding, H., Moser, C. C., Robertson, D. E., Tokito, M. K., Daldal, F., and Dutton, P. L. (1995) Ubiquinone pair in the Q_O site central to the primary energy conversion reactions of cytochrome bc_1 complex, *Biochemistry 34*, 15979−15996.

BI701905A